

# Efficient simulation of periodically forced reactors in 2-D

Bart van de Rotten<sup>a</sup>   Sjoerd Verduyn Lunel<sup>a</sup>   Alfred Blik<sup>b\*</sup>

## Abstract

The simulation of periodically forced processes in plug-flow reactors leads to the development of partial differential equations that are normally solved in time using dynamical simulation. Depending on the convergence properties of the system at hand, the number of cycles that needs to be computed up to a cyclic steady state is reached, can be large. Hence, direct iterative methods are essential. However, to overcome severe memory constraints many authors have reverted to pseudo-homogeneous one-dimensional models and to coarse grid discretization, which renders such models inadequate or inaccurate. In this paper we propose a limited memory iterative method, called the Broyden Rank Reduction method, to simulate a full two-dimensional model with radial gradients taken into account.

## Keywords

Numerical analysis; nonlinear dynamics; mathematical modeling; periodic processes; limited memory; reverse flow reactor.

## 1 Introduction

The reverse flow reactor (RFR) is a catalytic packed-bed reactor in which the flow direction is periodically reversed to trap a hot zone within the reactor. Upon entering the reactor, the cold feed gas is heated up regeneratively by the hot bed so that a reaction can occur. The reaction is assumed to be exothermic. At the other end of the reactor the hot product gas is cooled by the colder catalyst particles. The beginning and end of the reactor thus effectively work as heat exchangers. The cold feed gas purges the high-temperature (reaction) front in downstream direction. Before the hot reaction zone exits the reactor, the feed flow direction is reversed. The flow-reversal period, denoted by  $t_f$ , is usually constant and predefined. One complete RFR cycle consists of two flow-reverse periods. Overheating of the catalyst and hot spot formation are avoided by a limited degree of cooling. A schematic diagram of the reactor is shown in Figure 1.

Starting with an initial state, the reactor goes through a long transient phase before converging to a periodic limiting state, also called the cyclic steady state (CSS). Limiting states of periodically forced plug-flow reactors are industrially interesting because the reactor operates in this situation most of the time.

The basic model for a fixed bed catalytic reactor, such as the RFR, is the so-called pseudo-homogeneous one-dimensional model. This model does not differentiate between the fluid and the solid phase and considers gradients in the axial direction only.

Eigenberger and Nieken (1988) investigated a simplified one-dimensional model. Due to a very short residence time, they assumed the continuity equation and the mass balance equation to be in quasi steady state as compared to the energy balance equation. They applied standard dynamical simulation to compute the limiting periodic states of the reverse flow reactor. Due to their choice of the model and the values of the parameters all periodic states discovered were symmetric, that is, the state after one flow reversal period is the mirror image of the initial state.

---

<sup>a</sup> *Universiteit Leiden, Mathematical Institute, Niels Bohrweg 1, 2333 CA Leiden, The Netherlands*

<sup>b</sup> *Universiteit van Amsterdam, Institute for Chemical Engineering, Nieuwe Achtergracht 166, 1018 WV Amsterdam, The Netherlands*

\*Corresponding author. E-mail: blik@science.uva.nl, Fax: +31-20-525 5604

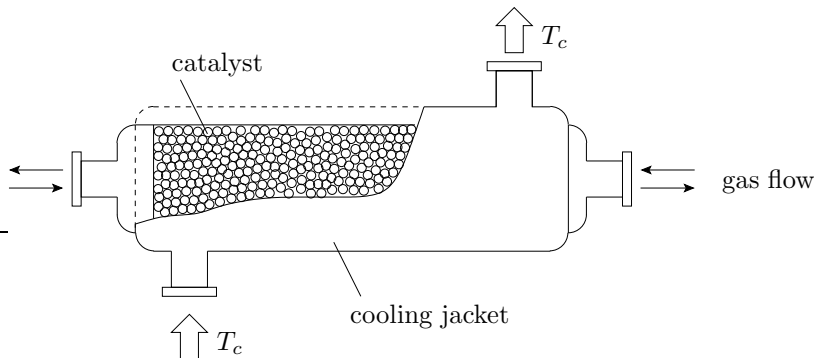


Figure 1: Schematic drawing of the cooled reverse flow reactor.

Rehacek, Kubicek and Marek (1992,1998) extended the model of the RFR to a two-phase model with mass- and energy transfer between the fluid and solid phase. They considered the period map, that is, the map which assigns to an initial state the new state after one period of the process. To obtain a numerical expression of the period map, the authors discretized the partial differential equations of the model in space and integrated the resulting system of ordinary differential equations over one period. Again with dynamical simulation, thus iterating the period map, symmetric stable periodic states of the RFR were obtained. In addition, they observed asymmetric and quasi-periodic behavior.

Khinast, Luss et al. (1997,1998,1999,2000) developed an efficient method to compute bifurcation diagrams of periodic processes. Their approach is based on previous work of Gupta and Bhatia (1991) in which the system of partial differential equations is considered as a boundary value problem in time. The boundary condition implies that the initial state of the reactor equals the state at the end of the cycle and, therefore, has to be a fixed point of the period map. The method of Broyden was used in combination with continuation techniques to find the parameter dependent fixed points of the period map.

For steady state processes that have coefficients and boundary conditions invariant in time, two-dimensional models are standard practice (Quinta Ferreira and Almeida-Costa, 1996). When modeling a steady state process, a time invariant state can often be expressed as the solution of a system of ordinary differential equations, where time derivatives are absent. For the theoretical analysis of limiting states of steady state processes, a great number of efficient mathematical and numerical tools is available. In periodically forced systems, such as the RFR, the limiting solution varies in time. To our knowledge, full two-dimensional models for the RFR have never been solved using a direct iterative method, such as the method of Broyden. The reason being that an accurate simulation requires a fine grid which yields a high dimensional discretized system. Due to large computational costs, both regarding CPU-time and regarding memory usage, two-dimensional models of periodically forced systems have so far been avoided, at the expense of relevance and accuracy.

The radial transport of heat and matter, however, is very important in non-isothermal packed bed reactors (Westertep, Swaaij and Beenackers, 1988). Highly exothermic reaction, a large width of the reactor, and efficient cooling of the reactor at the wall cause radial temperature gradients to be present, see Figure 2(b). Clearly, for cooled reverse flow reactors the radial dimension must explicitly be taken into account.

It is our aim to perform similar computations as done by Khinast, Jeong and Luss (1999), but now for the full two-dimensional model. However, a severe restriction of Broyden's method is the amount of memory needed to store the Broyden matrix. Therefore, we propose to use a new limited memory iterative method, called the Broyden Rank Reduction (BRR) method (Van de Rotten and Verduyn Lunel, 2003), which has the same rate of convergence as the method of Broyden, but uses far less memory. The BRR method is based on storing the most important information of the Broyden matrix in only two  $(n \times p)$ -matrices. So  $2pn$  storage locations are needed instead of  $n^2$  for the Broyden matrix. Here the parameter  $p$  can be chosen small and depends on the characteristics

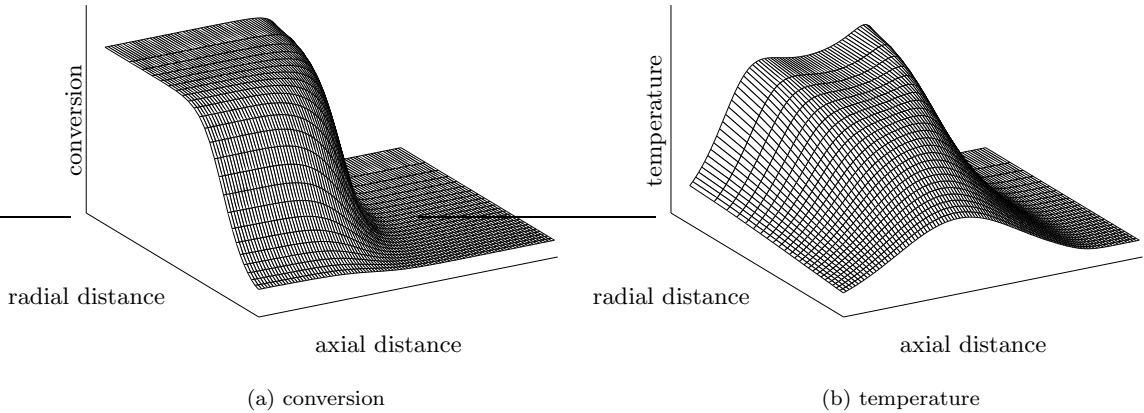


Figure 2: Qualitative temperature and conversion distribution of the cooled reverse flow reactor in the cyclic steady state using the two-dimensional model (4.5)-(4.7) with the parameter values of Tables 2 and 3.

of the process rather than on the dimension  $n$  of the discretized system.

As an example, we consider the two-dimensional model, see (4.5)-(4.7), for the reverse flow reactor and define  $f : \mathbb{R}^n \rightarrow \mathbb{R}^n$  to be the associated period map. We use 100 equidistant grid points in the axial direction and 25 grid points in the radial direction. The state vector, denoted by  $x$ , consist of the temperature and the concentration in every grid point. This implies that  $n = 5000$ . We apply the BRR method for different values of  $p$  to approximate a zero of the function  $g(x) = f(x) - x$  with a residue of  $10^{-8}$ . Figure 3 shows that the BRR method converges in 49 iterations for  $p = 10$ . Here, instead of 25,000,000 ( $n^2$ ) only 100,000 ( $2pn$ ) storage locations are needed for the Broyden matrix. If we permit a few more iterations,  $p$  can even be chosen equal to 5 and the number of storage locations can be reduced even further. If  $p$  is chosen too small ( $p = 2$ ) the (fast) convergence is lost. For complete details of the computations we refer to Section 5.

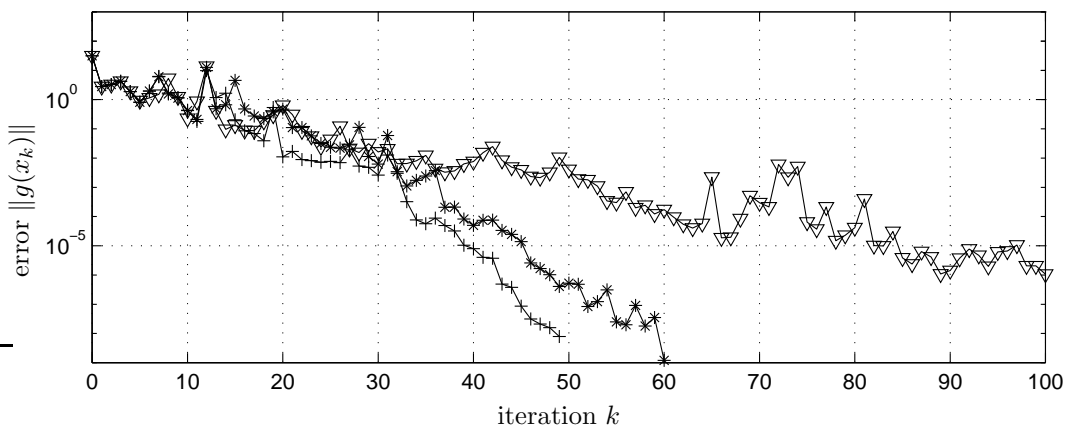


Figure 3: The convergence rate of the method of Broyden and the BRR method, for different values of  $p$ , applied to the period map of the reverse flow reactor using the two-dimensional model (4.5)-(4.7) with the parameter values of Tables 2 and 3. [ $+$ ] ( $p = 10$ ), [ $*$ ] ( $p = 5$ ), [ $\nabla$ ] ( $p = 2$ )]

The purpose of this article to present a direct iterative method, the Broyden Rank Reduction method, for the computation of periodic states of periodically forced processes. We describe a

complete simulation of the reverse flow reactor where radial temperature gradients are present and the radial dimension cannot be neglected.

## 2 The numerical procedure

Periodically forced processes in plug-flow reactors can be described by use of partial differential equations. In order to investigate the behavior of the system numerically, we discretize the equations in space using a finite volumes technique with first order upwind for the convective term. The state of the reactor at time  $t$  is denoted by a vector  $x(t)$  from the  $n$ -dimensional vector space,  $\mathbb{R}^n$ . The resulting system of  $n$  ordinary differential equations can be written as

$$x'(t) = F(x(t), t), \quad (2.1)$$

where  $F(\cdot, t + t_c) = F(\cdot, t)$  for  $t \in \mathbb{R}$ , and  $t_c$  denotes the period length.

The map  $f : \mathbb{R}^n \rightarrow \mathbb{R}^n$  that assigns to an initial state at time zero,  $x(0) = x_0$ , the value of the solution after one cycle,  $x(t_c)$ , is called the Poincaré or period map of (2.1). So we have

$$f(x_0) = x(t_c). \quad (2.2)$$

In other words, evaluating the map  $f$  is equivalent to simulating one cycle of the process in (2.1).

A periodic state of the reactor corresponds to a  $t_c$ -periodic solution  $x(t)$  of (2.1). Since the initial condition,  $x_0$ , of a periodic solution is a fixed point of the period map, we solve

$$g(x) = f(x) - x = 0, \quad (2.3)$$

using iterative methods. Note that the value  $f(x)$  is obtained by integrating a large system of ordinary differential equations over a period  $t_c$ . Therefore the function evaluation is a computationally expensive task, and the iterative method that needs the fewest evaluations of  $f$  to solve (2.3), is the most efficient. Since it might take a long transient time before the limiting state is reached, direct methods are preferable to dynamical simulation. Van Noorden (2002a,2002b) compared several convergence acceleration techniques, such as the methods of Newton and Broyden, and the newly developed Newton-Picard method (Lust et al., 1998; Van Noorden, Verduyn Lunel and Blik, 2003). From the work of Van Noorden et al., it turns out that Broyden's method is the most efficient for solving large systems of nonlinear equations in terms of function evaluations.

In order to determine the stability of a fixed point we compute the Floquet multipliers of the system, i.e., the eigenvalues of the Jacobian of  $f$  ( $J_f$ ) at the fixed point. If all Floquet multipliers are inside the unit circle of the complex plane the fixed point is stable (Iooss and Joseph, 1990).

## 3 The Broyden Rank Reduction method

The limitation of direct iterative method to simulate models of the reverse flow reactor is the usage of an  $(n \times n)$ -matrix to accelerate the convergence. To overcome severe memory constraints, so far, only simplified models have been considered. In this section we present a new direct iterative method, called the Broyden Rank Reduction (BRR) method, that uses far less memory. Before we give the description of the BRR method, we first recall the method of Broyden (Broyden, 1965).

**Algorithm 3.1 (The method of Broyden)** Choose an initial estimate  $x_0 \in \mathbb{R}^n$  and an initial Broyden matrix  $B_0$ . Set  $k := 0$  and repeat the following sequence of steps until  $\|g(x_k)\| < \varepsilon$ .

- i) Solve  $B_k s_k = -g(x_k)$  for  $s_k$ ,
- ii)  $x_{k+1} := x_k + s_k$ ,
- iii)  $y_k := g(x_{k+1}) - g(x_k)$ ,
- iv)  $B_{k+1} := B_k + (y_k - B_k s_k) s_k^T / (s_k^T s_k)$ ,
- v) Increase  $k$  by one.

According to step (iv) of Algorithm 3.1, the Broyden matrix in the  $p$ th iteration can be written as

$$B_p = B_0 + \sum_{k=0}^{p-1} (y_k - B_k s_k) s_k^T / (s_k^T s_k) = B_0 + CD^T, \quad (3.1)$$

where  $C = [c_1 \cdots c_p]$  and  $D = [d_1 \cdots d_p]$  contain the updates to the Broyden matrix, that is, for  $k = 0, \dots, p-1$ ,

$$c_{k+1} = (y_k - B_k s_k) / \|s_k\|, \quad \text{and} \quad d_{k+1} = s_k / \|s_k\|. \quad (3.2)$$

By choosing  $B_0$  to be minus the identity ( $B_0 = -I$ ), the initial Broyden matrix can be implemented in the code. So it suffices to store the matrices  $C$  and  $D$ . In order to keep the number of columns of  $C$  and  $D$  fixed at  $p$  in all subsequent iterations a reduction procedure is applied to the update matrix  $CD^T$ . This allows the storage of a new update to the Broyden matrix in  $C$  and  $D$  in every next iteration. In summary, we have the following description of the BRR algorithm.

**Algorithm 3.2 (The Broyden Rank Reduction method)** Choose an initial estimate  $x_0 \in \mathbb{R}^n$ , set the parameter  $p$ , and let  $C = [c_1 \cdots c_p]$ ,  $D = [d_1 \cdots d_p] \in \mathbb{R}^{n \times p}$  be initialized by  $c_i = d_i = 0$  for  $i = 1, \dots, p$ . Set  $k := 0$  and repeat the following sequence of steps until  $\|g(x_k)\| < \varepsilon$ .

- i) Solve  $(I - D^T C)t_k = -D^T g(x_k)$  for  $t_k$ ,
- ii)  $s_k := -g(x_k) + Ct_k$ ,
- iii)  $x_{k+1} := x_k + s_k$ ,
- iv)  $y_k := g(x_{k+1}) - g(x_k)$ ,
- v) Compute the QR-decomposition of  $D = QR$ , where  $Q$  is an orthogonal  $(n \times p)$ -matrix and  $R$  an upper triangular  $(p \times p)$ -matrix,  
 $D := Q, \quad C := CR^T$ ,
- vi) Compute the singular value decomposition of  $C = U\Sigma W^T$ , where  $U, W$  are orthogonal  $(n \times p)$ -matrices and  $\Sigma = \text{diag}(\sigma_1, \dots, \sigma_p)$ , where  $\sigma_1 \geq \dots \geq \sigma_p \geq 0$ ,  
 $C := U\Sigma, \quad D := DW$ ,
- vii)  $c_p := (y_k - (-I + CD^T)s_k) / \|s_k\|$ , and  $d_p := s_k / \|s_k\|$ ,
- viii) Increase  $k$  by one.

Note that in step (v) of the first iteration of Algorithm 3.2 the QR-decomposition is computed of a zero matrix. Since, however, the matrix  $R$  is then set to zero, we can choose any orthogonal matrix  $Q$  without disturbing the procedure. The update to the Broyden matrix is always stored in the last columns of the matrices  $C$  and  $D$ . In the next iteration, these matrices  $C$  and  $D$  are replaced by the factors of the singular value decomposition of the update matrix  $CD^T$ . Note that the singular values are ordered in decreasing order. Therefore, after step (vi) of the second iteration of the BRR method the first update to the Broyden matrix is stored in the first columns of  $C$  and  $D$ . In addition, after  $p$  iterations of the BRR method the  $p$ th singular value is automatically removed in every iteration.

According to Algorithm 3.2, the singular value decomposition of  $CD^T$  is actually computed without forming the large  $(n \times n)$ -matrix. Due to the Sherman and Morrison formula (cf. Dennis and Schnabel, 1983), it suffices to solve a  $p$ -dimensional system for the computation of the Broyden step  $s_k$  in (i) and (ii) of Algorithm 3.2. The convergence properties of the BRR method are described in full detail by Van de Rotten and Verduyn Lunel (2003). The BRR method turns out to be an ideal iterative method to simulate periodically forced processes in plug flow reactors.

## 4 Derivation of the two-dimensional model

In this section we describe the two-dimensional model mentioned in the introduction, that will be the basis of our simulations in Section 6. Starting from the one-dimensional pseudo-homogeneous model of Khinast, Jeong and Luss (1999), we incorporate the radial direction. In the one-dimensional model of Khinast et al. axial heat and mass dispersion are accounted for. It is assumed that all the physical properties are independent of the temperature and concentration and that the pressure loss along the length of the catalytic bed is negligible. The component balance contains diffusion, convection and reaction terms and reads

$$\varepsilon \frac{\partial c}{\partial t} = \varepsilon D_{\text{ax}} \frac{\partial^2 c}{\partial z^2} - u \frac{\partial c}{\partial z} - r'(c, T), \quad (4.1)$$

where the reaction rate is given by

$$r'(c, T) = \frac{\eta k_{\infty} a_v k_c \exp[-E_a/R_{\text{gas}}T]}{a_v k_c + \eta k_{\infty} \exp[-E_a/R_{\text{gas}}T]} c.$$

The energy balance involves a cooling term and is given by

$$((\rho c_p)_s(1 - \varepsilon) + (\rho c_p)_g \varepsilon) \frac{\partial T}{\partial t} = \lambda_{\text{ax}} \frac{\partial^2 T}{\partial z^2} - u(\rho c_p)_g \frac{\partial T}{\partial z} + (-\Delta H)r'(c, T) - U_w a_w (T - T_c). \quad (4.2)$$

From the assumption that diffusion occurs only inside the reactor, it follows that Danckwerts boundary conditions are valid at both ends of the reactor. So

$$\begin{aligned} -\lambda_{\text{ax}} \frac{\partial T}{\partial z} \Big|_{z=0} &= u(\rho c_p)_g (T_0 - T(0)), & \frac{\partial T}{\partial z} \Big|_{z=L} &= 0, \\ -\varepsilon D_{\text{ax}} \frac{\partial c}{\partial z} \Big|_{z=0} &= u(c_0 - c(0)), & \frac{\partial c}{\partial z} \Big|_{z=L} &= 0. \end{aligned} \quad (4.3)$$

To extend the one-dimensional model from Khinast, Jeong and Luss (1999) with the radial direction, we follow the assumptions proposed by Westerterp, Swaaij and Beenackers (1988),

- (1) The state of the reactor is cylindrically symmetric,
- (2) The diffusion coefficients  $D_{\text{rad}}$  and  $\lambda_{\text{rad}}$  are independent of position, concentration and temperature.

These assumptions lead to the following adjustments to the one-dimensional model. The concentration and temperature depend on the axial and the radial direction,  $c = c(z, r, t)$  and  $T = T(z, r, t)$ . The second spatial dimension is incorporated by including the radial components of the diffusion terms,

$$\varepsilon D_{\text{rad}} \frac{1}{r} \frac{\partial}{\partial r} \left\{ r \frac{\partial c}{\partial r} \right\} \quad \text{and} \quad \lambda_{\text{rad}} \frac{1}{r} \frac{\partial}{\partial r} \left\{ r \frac{\partial T}{\partial r} \right\},$$

in the component balance and the energy balance, respectively. The cooling term in the energy balance disappears. Instead, at the wall of the reactor the boundary condition

$$\lambda_{\text{rad}} \frac{\partial T}{\partial r} \Big|_{r=R} = -U_w (T(R) - T_c), \quad (4.4)$$

is added to the system. Equation (4.4) describes the heat loss at the reactor wall to the surrounding cooling jacket. The cooling jacket is assumed to be kept at constant temperature  $T_c$  and, therefore, the cooling temperature is assumed to be independent of the axial distance. Because no material can pass through the wall of the reactor, we have

$$\frac{\partial c}{\partial r} \Big|_{r=R} = 0.$$

The cylindrical symmetry in the reactor yields the boundary conditions

$$\frac{\partial c}{\partial r} \Big|_{r=0} = 0, \quad \text{and} \quad \frac{\partial T}{\partial r} \Big|_{r=0} = 0.$$

In summary we can now give the complete two-dimensional model. The component balance is given by

$$\varepsilon \frac{\partial c}{\partial t} = \varepsilon D_{\text{ax}} \frac{\partial^2 c}{\partial z^2} - u \frac{\partial c}{\partial z} - r'(c, T) + \varepsilon D_{\text{rad}} \frac{1}{r} \frac{\partial}{\partial r} \left\{ r \frac{\partial c}{\partial r} \right\}, \quad (4.5)$$

the energy balance is given by

$$\begin{aligned} ((\rho c_p)_s(1 - \varepsilon) + (\rho c_p)_g \varepsilon) \frac{\partial T}{\partial t} = \lambda_{\text{ax}} \frac{\partial^2 T}{\partial z^2} - u(\rho c_p)_g \frac{\partial T}{\partial z} + \\ (-\Delta H)r'(c, T) + \lambda_{\text{rad}} \frac{1}{r} \frac{\partial}{\partial r} \left\{ r \frac{\partial T}{\partial r} \right\}, \end{aligned} \quad (4.6)$$

and the boundary conditions are given by

$$\begin{aligned} -\lambda_{\text{ax}} \frac{\partial T}{\partial z} \Big|_{z=0} &= u(\rho c_p)_g (T_0 - T(0)), & \frac{\partial T}{\partial z} \Big|_{z=L} &= 0, \\ -\varepsilon D_{\text{ax}} \frac{\partial c}{\partial z} \Big|_{z=0} &= u(c_0 - c(0)), & \frac{\partial c}{\partial z} \Big|_{z=L} &= 0, \\ \frac{\partial c}{\partial r} \Big|_{r=0} &= 0, & \frac{\partial c}{\partial r} \Big|_{r=R} &= 0, \\ \frac{\partial T}{\partial r} \Big|_{r=0} &= 0, & \lambda_{\text{rad}} \frac{\partial T}{\partial r} \Big|_{r=R} &= -U_w(T(R) - T_c). \end{aligned} \quad (4.7)$$

The values of the parameters in this model are given in Tables 2 and 3.

Before doing simulations with the two-dimensional model (4.5)-(4.7), we simplify the problem in the following way. From the mathematical point of view, it makes no difference if the flow direction in the reactor is reversed or if the reactor is reversed itself while the fluid flows from the same direction. Therefore we do not compute the state of the RFR after a whole cycle, but we integrate the system over one flow reverse period ( $t_f$ ) and then reverse the reactor in the axial direction. Thus, instead of (2.2), the period map is given by

$$f(x) = x(L - z, t_f), \quad (4.8)$$

where  $L$  is length of the reactor. The state of the reactor after a whole cycle is then obtained by applying the map  $f$  twice to the initial condition. A fixed point of  $f$  corresponds to a symmetric periodic state of the reactor. If asymmetric periodic states exist, we can find them by computing fixed points of the original period map. The only way to determine whether the limiting state of the reactor is quasi-periodic is by using dynamical simulation. In this article we restrict ourselves to the computation of symmetric periodic states.

## Justification of the two-dimensional model

In the following, we justify that the above extension of the one-dimensional model is indeed natural. The relation between the one- and two-dimensional balance equations is based on the idea of a weighted average. To give a useful one-dimensional representation of the two-dimensional state of the reactor, the weighted average can be taken of the temperature and the concentration over the cross section of the reactor. In the two-dimensional model, we have denoted the temperature in the point  $(z, r)$  at time  $t$  by  $T(z, r, t)$ . So the average temperature over the cross section through  $z = z_0$  equals

$$\bar{T}(z_0, t) = \frac{2}{R^2} \int_0^R r T(z_0, r, t) dr. \quad (4.9)$$

If we take the weighted average of both sides of the energy balance, (4.6), over the cross section of the reactor and use (4.9) for the weighted average of the temperature, then we obtain

$$\begin{aligned} ((\rho c_p)_s(1 - \varepsilon) + (\rho c_p)_g \varepsilon) \frac{\partial \bar{T}}{\partial t} = \lambda_{\text{ax}} \frac{\partial^2 \bar{T}}{\partial z^2} - u(\rho c_p)_g \frac{\partial \bar{T}}{\partial z} + \\ (-\Delta H) \frac{2}{R^2} \int_0^R r \cdot r'(c, T) dr + \lambda_{\text{rad}} \frac{2}{R^2} r \frac{\partial T}{\partial r} \Big|_{r=0}^R. \end{aligned} \quad (4.10)$$

Using the last two boundary conditions listed in (4.7), we can rewrite the last term of (4.10) as follows

$$\lambda_{\text{rad}} \frac{2}{R^2} r \frac{\partial T}{\partial r} \Big|_{r=0}^R = -\frac{2}{R} U_w (T(R) - T_0). \quad (4.11)$$

If we substitute (4.11) in (4.10) and assume that the concentration and the temperature are constant in the radial direction, we recover the energy balance of the one-dimensional model, (4.2), with  $a_w = \frac{2}{R}$ .

In the same way we can show that the component balance of the one-dimensional model, (4.1), is also a limiting case of our the component balance of the two-dimensional model, (4.5).

## 5 Finer grid using same amount of memory

In this section we use the BRR method to find symmetric periodic solutions of the RFR using the full two-dimensional model of the RFR. In addition, we show that even when using the one-dimensional description of the RFR, the BRR method saves memory. It turns out that, surprisingly, for the two-dimensional model the same values for  $p$  can be used as in case of the one-dimensional model. Finally, we show that it is possible to use a finer grid with the same amount of memory to store the Broyden matrix at the expense of just a few more iterations.

### The one-dimensional model

Let  $f : \mathbb{R}^n \rightarrow \mathbb{R}^n$  be the map of one flow reverse period, see (4.8), that corresponds to the balance equations in (4.1)-(4.3) using the parameters values of Table 2. In addition, we fix the flow reverse period and the dimensionless cooling capacity ( $t_f = 1200\text{s}$  and  $\Phi = 0.2$ ). As initial condition we take a state of the reactor that is at high constant temperature ( $T = 2T_0$ ) and filled with inert gas ( $c = 0$ ). For the finite volume discretization an equidistant grid is used with  $N$  grid points ( $N = 100$ ). This leads to an  $n$ -dimensional discretized problem ( $n = 2N = 200$ ). The system of ordinary differential equations is integrated over one reverse flow period using the NAG-library routine D02EJF. To solve the equation  $g(x) = 0$  with  $g(x) = f(x) - x$ , the BRR method is applied for different values of  $p$ .

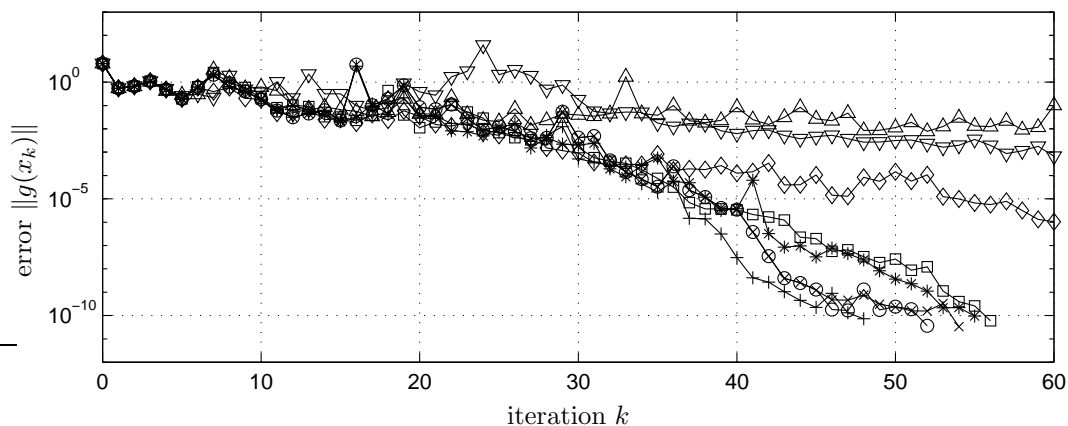


Figure 4: The convergence rate of the method of Broyden and the BRR method, for different values of  $p$ , applied to the period map of the reverse flow reactor using the one-dimensional model (4.1)-(4.3) with the parameter values of Table 2. [ $'o'$  (Broyden),  $'x'$  ( $p = 20$ ),  $'+'$  ( $p = 10$ ),  $'*'$  ( $p = 5$ ),  $'v'$  ( $p = 4$ ),  $'\diamond'$  ( $p = 3$ ),  $'\nabla'$  ( $p = 2$ ),  $'\triangle'$  ( $p = 1$ )]

The information in Figure 4 can be interpreted as follows. The method of Broyden converges up to a residue with  $\|g(x_k)\| < 10^{-10}$  in 52 iterations. For  $p = 20$ , the BRR method is approximately as fast as the method of Broyden using one fifth of the amount of memory. Note that the residues of both methods are equal up to the 45th iteration. For  $p = 10$ , the BRR method is even faster than

the method of Broyden. Thus The number of iterations needed to converge up to  $\|g(x_k)\| < 10^{-10}$  is not monotonously increasing for smaller values of  $p$ . If we take  $p = 5$  or  $p = 4$  instead of  $p = 10$ , the BRR method needs a few more iterations to converge. Note, however, that then the amount of memory needed is divided by a factor 2 and  $\frac{5}{2}$ , respectively. For  $p = 3$ ,  $p = 2$ , and  $p = 1$  the BRR method has a very low rate of convergence. We see that with just a few more iterations a large reduction of memory is obtained.

## The two-dimensional model

Let  $f : \mathbb{R}^n \rightarrow \mathbb{R}^n$  now be the map of one flow reverse period, see (4.8), corresponding to the balance equations in (4.5)-(4.7) using the parameters values of Tables 2 and 3. Again, we fix the flow reverse period and the dimensionless cooling capacity ( $t_f = 1200\text{s}$  and  $\Phi = 0.2$ ). The ratio between the width and the length of the reactor is set at  $R/L = 0.0025$ . As initial condition again a state of the reactor is taken that is at high constant temperature ( $T = 2T_0$ ) and filled with inert gas ( $c = 0$ ). For the finite volume discretization an equidistant grid is used with  $N$  grid points in the axial direction ( $N = 100$ ). In the radial direction a non-uniform grid of  $M$  grid points is chosen that becomes finer in the direction of the wall of the reactor ( $M = 25$ ). In fact, a segment of the reactor is divided in  $M$  rings with the same volume. The dimension of the discretized problem is again denoted by  $n$  ( $n = 2 \cdot M \cdot N = 5000$ ). The system of ordinary differential equations is integrated over one reverse flow period using the NAG-library routine D02NCF.

To solve the equation  $g(x) = 0$ , with  $g(x) = f(x) - x$ , the BRR method is applied for different values of  $p$ . It turns out that for the two-dimensional model it is no longer possible to apply Broyden's method directly, due to memory constraints.

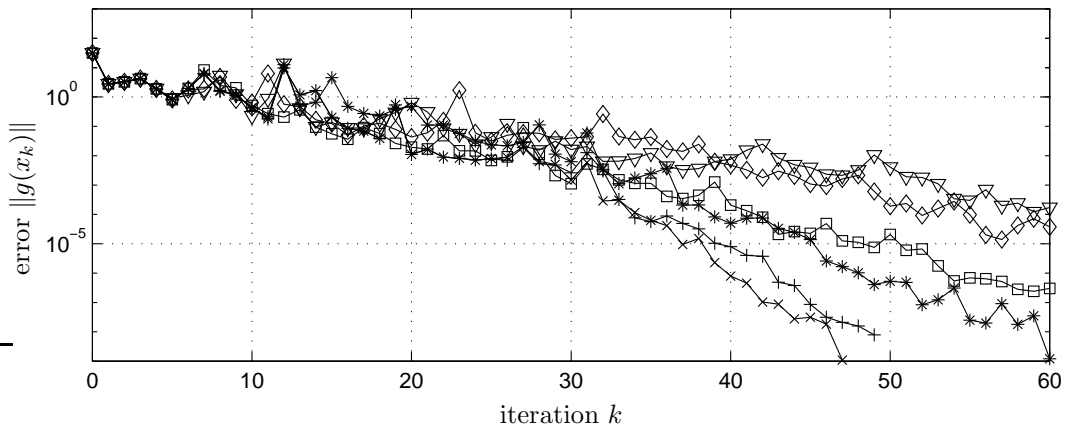


Figure 5: The convergence rate of the BRR method, for different values of  $p$ , applied to the period map of the reverse flow reactor using the two-dimensional model (4.5)-(4.7) with the parameter values of Tables 2 and 3. [ $\times$ ' ( $p = 20$ ),  $+$ ' ( $p = 10$ ),  $*$ ' ( $p = 5$ ),  $\square$ ' ( $p = 4$ ),  $\diamond$ ' ( $p = 3$ ),  $\nabla$ ' ( $p = 2$ )]

Figure 5 shows that the BRR method has a high rate of convergence for  $p \geq 5$ . For  $2 \leq p \leq 4$  the BRR method does not converge within 60 iterations. The amount of memory needed to store the Broyden matrix can be reduced by choosing  $p = 10$  instead of  $p = 20$ , using approximately the same number of iterations.

For the above simulation of the two-dimensional model a very slim reactor is used ( $R/L = 0.0025$ ). As will be discussed Section 6, gradients in the radial direction are absent in this case, and the two-dimensional model leads to exactly the same results as the one-dimensional model. If we take a larger radius for the reactor ( $R/L = 0.025$ ), then radial temperature gradients are in fact introduced. To illustrate the benefits of our limiting memory method we compare two simulations of the model with  $M = 25$  and  $M = 5$  grid points in the radial direction. So the dimension of the discretized problem becomes  $n = 5000$  and  $n = 1000$ , respectively.

We have applied the BRR method with different values of  $p$  to compute the periodic state of the reactor, see Table 1.

|          | $M = 25$     |                     | $M = 5$      |                     |
|----------|--------------|---------------------|--------------|---------------------|
|          | # iterations | # storage locations | # iterations | # storage locations |
| $p = 20$ | 48           | 200,000             | 53           | 40,000              |
| $p = 10$ | 50           | 100,000             | 55           | 20,000              |
| $p = 5$  | 61           | 50,000              | 65           | 10,000              |
| $p = 4$  | 65           | 40,000              | 82           | 8,000               |
| $p = 3$  | 80           | 30,000              | 76           | 6,000               |
| $p = 2$  | > 100        | 20,000              | 90           | 4,000               |
| $p = 1$  | > 100        | 10,000              | > 100        | 2,000               |

Table 1: The number of iterations to solve (2.3), corresponding to the two-dimensional problem, needed by the BRR method for different values of  $p$  and the number of storage locations for the Broyden matrix using a grid with  $N = 100$  grid points in the axial direction and  $M = 25$ , respectively  $M = 5$ , grid points in the radial direction.

Although a few more iterations are needed than in case of the slim reactor ( $R/L = 0.0025$ ), still the same values for  $p$  can be used for both the fine and the coarse grid. Note that for every value of  $p$  the convergence for  $M = 25$  is faster than for  $M = 5$ . Suppose, however, that at most 40,000 storage locations are available. To accelerate the convergence we want to use the largest value of  $p$ . For the coarse grid  $p$  can be chosen to be 20 and for the fine grid at most  $p = 4$ . This implies that instead of 53 iterations for a coarse grid, 65 iterations are needed for a fine grid to solve the discretized problem while using the same amount of memory to store the Broyden matrix.

Although the approximation of the cyclic steady state is qualitatively good using the coarse grid, Figure (6(a)), the more accurate approximation using the fine grid, Figure (6(b)), is preferable.

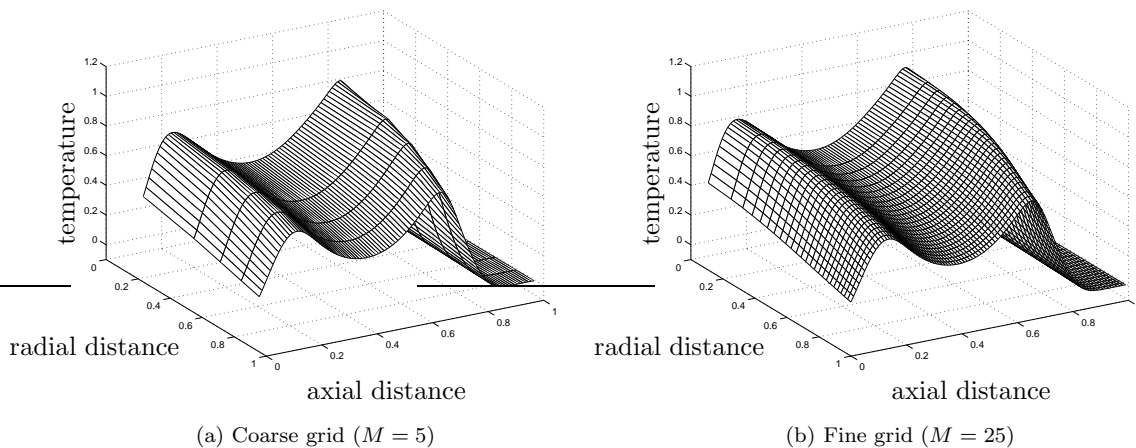


Figure 6: Temperature distribution over the reactor bed using a coarse and a fine grid.

## 6 Dynamic features of the two-dimensional model

In this section we consider aspects of limiting periodic states of the RFR for different values of the dimensionless reactor radius, denoted by  $R/L$ . The results are expressed in the dimensionless temperature  $(T - T_0)/T_0$  and the conversion  $(c_0 - c)/c_0$ . We have fixed the flow reverse period

( $t_f = 1200s$ ). As a bifurcation parameter we use the dimensionless cooling capacity, defined by,

$$\Phi = \frac{2LU_w}{Ru(\rho c_p)_g}. \quad (6.1)$$

To obtain the results of this section the BRR method is used with  $p = 30$ . The bifurcation diagrams, describing the dependence of the symmetric periodic state of the reactor on the dimensionless cooling capacity, are constructed using a standard continuation technique in combination with the BRR method. Eigenvalues of  $J_f$  are determined using the subspace method with locking (Saad, 1992).

We describe two different cases of the limiting periodic state for a fixed value of the cooling capacity ( $\Phi = 0.2$ ). If the reactor is rather slim (for example,  $R/L = 0.0025$ ), we observe that the temperature is constant over every cross section of the reactor, see Figure 7(b). In this way we can validate the two-dimensional model. Indeed according to the theory of Section 4, if radial gradients are absent, the weighted average of the two-dimensional temperature profile equals the temperature profile of the one-dimensional model. This has been confirmed by simulations of the one-dimensional model. The same observation is valid for the conversion, see Figure 7(a).

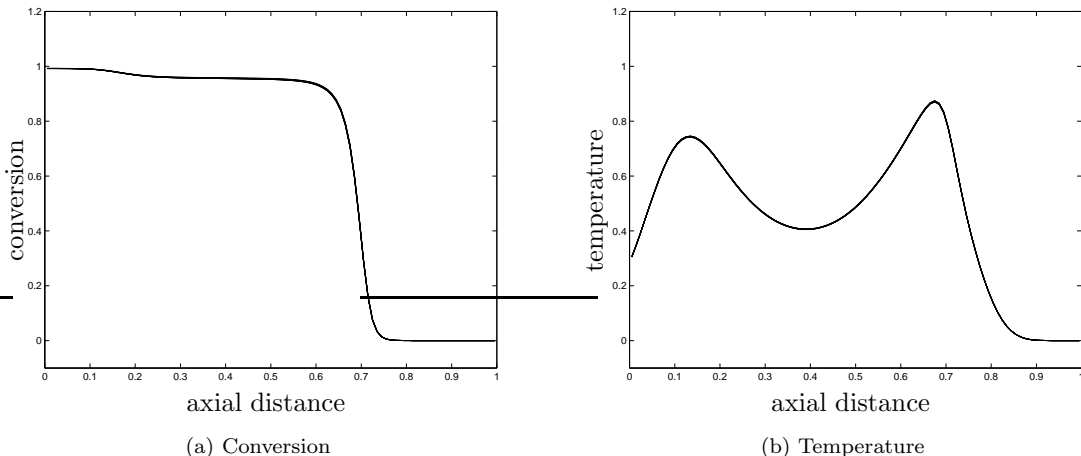


Figure 7: Axial temperature and conversion profiles of the RFR (in CSS) at the beginning of a reverse flow period using the two-dimensional model (4.5)-(4.7) with the parameter values of Tables 2 and 3. The cooling capacity  $\Phi$  is fixed at 0.2 and the radius of the reactor equals  $R/L = 0.0025$ .

We use the same value for the cooling capacity ( $\Phi = 0.2$ ), but now with a larger reactor width ( $R/L = 0.025$ ). This implies that the cooling now propagates less easily through the reactor and steep temperature gradients in the radial direction arise. In Figure 8(b) we have represented the distribution of the temperature over the catalyst bed in the cyclic steady state. For several positions in the radial direction, the temperature profile along the reactor is plotted. The lines with the highest temperatures correspond to radial positions near the axis of the reactor. The lines with the lowest temperature correspond to radial positions near the wall of the reactor. Clearly, the cooling is especially influencing the temperature of the catalyst near the wall of the reactor. Note that for different radial positions the axial position of the maximum temperature is shifted. This results in a lower maximum of the weighted average of the temperature. In Figure 8(a) the conversion of the same cyclic steady state is given. The lines with the highest conversion correspond to radial positions near the axis of the reactor. The lines with the lowest conversion correspond to radial positions near the wall of the reactor. Note that only around the axis the conversion is complete at the end of the reactor. Therefore the product gas consists of a mixture of both products as reactants and on an average the conversion is not complete.

Two bifurcation branches are shown in Figure 9. The maximum (weighted averaged) temperature is plotted versus the dimensionless cooling capacity  $\Phi$  for different values of  $R/L$ . It can be

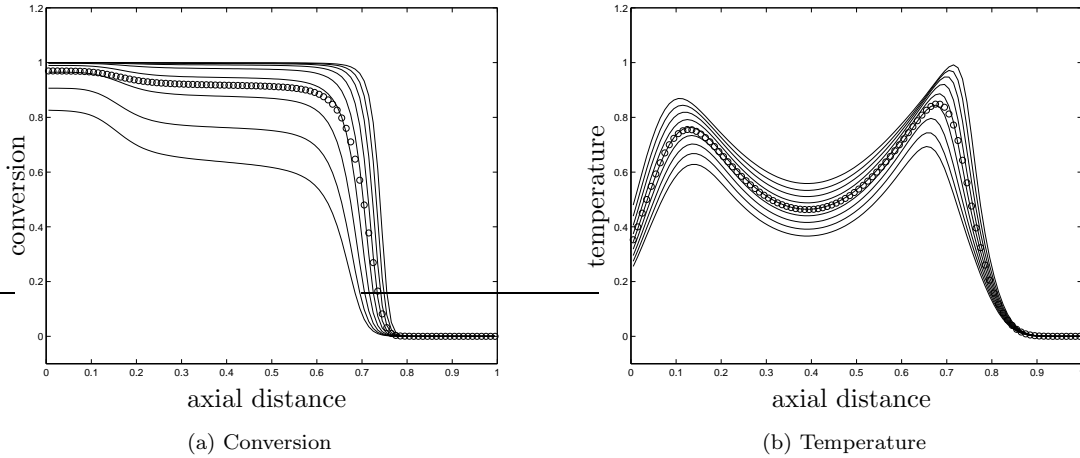


Figure 8: Axial temperature and conversion profiles of the RFR (in CSS) at the beginning of a reverse flow period using the two-dimensional model (4.5)-(4.7) with the parameter values of Tables 2 and 3. The cooling capacity  $\Phi$  is fixed at 0.2 and the radius of the reactor equals  $R/L = 0.025$ . In addition, the weighted average (4.9) is given ('o').

shown that, for every value of the cooling capacity, a stable extinguished state exists. For the slim reactor ( $R/L = 0.0025$ ) the maximum average temperature is always higher than for the wide reactor ( $R/L = 0.025$ ) at the same cooling capacity. This can be explained by the fact that for the wide reactor, for different radial positions, the maximum of the temperature is not found at the same axial position in the reactor. Note that for the slim reactor there exists a minimum in the upper branch (at  $\Phi \approx 0.3$ ). The reason being the two high temperature zones, cf. Figure 7(b), merge into one. For cooling capacities higher than  $\Phi \approx 0.67$ , the reactor cannot operate at high temperature and dies out. The part of the branch with negative cooling capacity has of course no physical meaning. The bifurcation branch for the wide reactor has more or less the same characteristics. However, the minimum has disappeared and the upper branch has become monotonically decreasing.

To determine the stability of the points on the bifurcation branches, we have also plotted the largest Floquet multiplier ( $\mu_{\max}$ ) in Figure 9. Starting with  $\Phi = 0$  at the upper branch of the bifurcation diagram the largest eigenvalue of the Jacobian at the fixed points is slightly less than +1, implying that the fixed points are stable. At  $\Phi \approx 0.15$  ( $\Phi \approx 0.16$  for the wide reactor) a negative eigenvalue becomes larger and crosses the unit circle at  $\mu = -1$  for  $\Phi \approx 0.19$  ( $\Phi \approx 0.18$  for the wide reactor), causing a symmetry loss bifurcation, that is, the symmetric state become unstable and a stable asymmetric period-1 state emerges. For cooling capacities higher than  $\Phi \approx 0.32$  ( $\Phi \approx 0.48$ ), the largest eigenvalue returns to the unit circle but remains close to  $-1$ . Then the symmetric state is stable but it takes the reactor a large number of cycles to converge to this limiting state. Finally, at the limit point, for which  $\Phi \approx 0.67$  ( $\Phi \approx 0.65$ ), a positive eigenvalue crosses the unit circle at  $\mu = +1$ . Thus for higher cooling capacities, the cooling eventually causes extinction of the reactor. The fixed points of the lower branches for both the wide and the slim reactor are unstable.

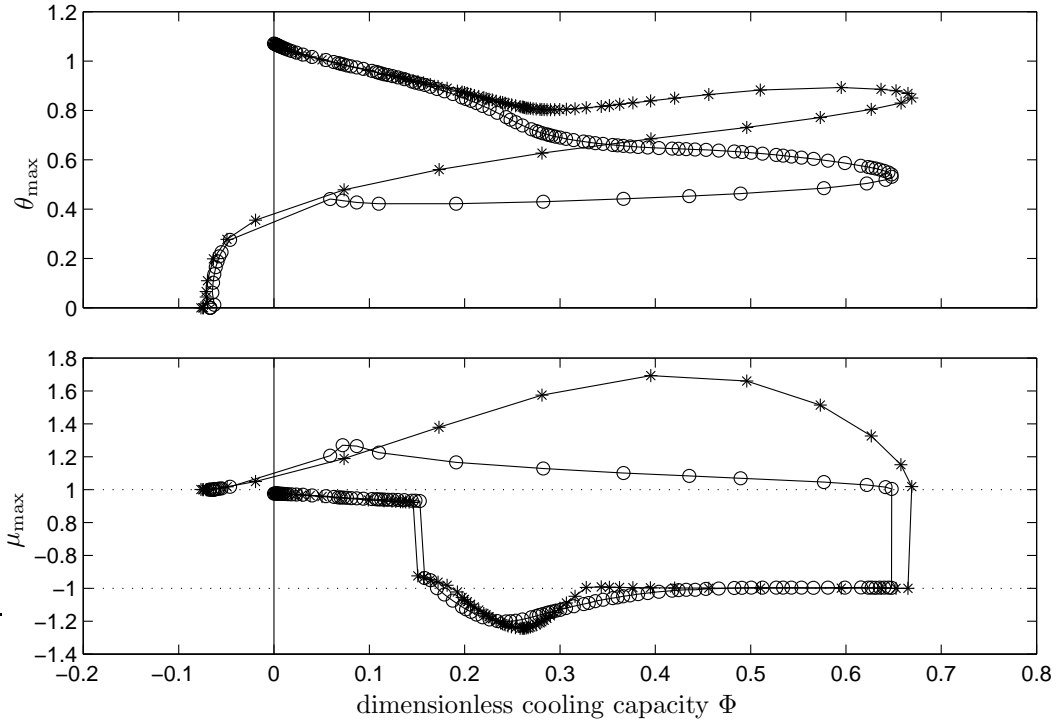


Figure 9: The maximum dimensionless temperature ( $\theta_{\max}$ ) and the largest Floquet multiplier ( $\mu_{\max}$ ) versus the cooling capacity ( $\Phi$ ) for two different values of the reactor radius. The two-dimensional model (4.5)-(4.7) was used with the parameter values of Tables 2 and 3. ['\*' ( $R/L = 0.0025$ ), 'o' ( $R = 0.025$ )]

## 7 Conclusions

The excessive computational effort in deriving cyclic steady state results for 2-D periodic reactors has forced researchers to either neglect two-dimensional effects or to simplify models for instance to quasi two-dimensional models. Using the example of a cooled reverse flow reactor for exothermic reactions, we have demonstrated that it is indeed possible to use a full two-dimensional model, while still circumventing the use of excessive computational time and memory. For this we used our new limited memory Broyden method, that reduces the number of locations to store the Broyden matrix significantly. We have also demonstrated that this method allows one to carry out a bifurcation analysis.

# Symbols

## Roman

|                  |   |
|------------------|---|
| $a_v$            | specific external particle surface area, $\text{m}_{\text{surf}}^2/\text{m}_{\text{reactor}}^3$ |
| $a_w$            | specific reactor wall surface area, $\text{m}_{\text{wall}}^2/\text{m}_{\text{reactor}}^3$      |
| $c$              | concentration, $\text{kmol}/\text{m}^3$   |
| $D$              | dispersion coefficient, $\text{m}^2/\text{s}$   |
| $d_p$            | particle diameter, $\text{m}$   |
| $E_a$            | activation energy, $\text{kJ}/\text{kmol}$  |
| $h$              | heat-transfer coefficient, $\text{kW}/(\text{m}^2 \text{K})$                                    |
| $k_c$            | mass-transfer coefficient, $\text{m}/\text{s}$  |
| $k_\infty$       | frequency factor for reaction, $\text{s}^{-1}$  |
| $L$              | reactor length, $\text{m}$  |
| $r$              | radial distance, $\text{m}$   |
| $R$              | radius of the reactor, $\text{m}$   |
| $R_{\text{gas}}$ | universal gas constant, $\text{kJ}/(\text{kmol K})$   |
| $u$              | superficial gas velocity, $\text{m}/\text{s}$   |
| $U_w$            | heat-transfer coefficient at reactor wall, $\text{kW}/(\text{m}^2 \text{K})$                    |
| $t$              | time, $\text{s}$  |
| $t_f$            | flow reverse time, $\text{s}$   |
| $T$              | temperature, $\text{K}$   |
| $T_c(T_0)$       | cooling(feed) temperature, $\text{K}$   |
| $z$              | axial distance, $\text{m}$  |

## Greek

|                         |   |
|-------------------------|---|
| $-\Delta H$             | heat of reaction, $\text{kJ}/\text{kmol}$                           |
| $-\Delta T_{\text{ad}}$ | adiabatic temperature rise, $\text{K}$                              |
| $\varepsilon$           | void fraction, $[-]$  |
| $\eta$                  | effectiveness factor, $[-]$   |
| $\lambda_0$             | (isotropic) thermal conductivity, $\text{kW}/(\text{m}^3 \text{K})$ |
| $\lambda'$              | convective heat conductivity, $\text{kW}/(\text{m}^3 \text{K})$     |
| $\lambda$               | thermal conductivity, $\text{kW}/(\text{m}^3 \text{K})$             |
| $(\rho c_p)$            | volumetric heat capacity, $\text{kJ}/(\text{m}^3 \text{K})$         |
| $\Phi$                  | dimensionless cooling capacity, $[-]$                               |

## Dimensionless parameters

|    |                   |
|----|-------------------|
| Bo | Bodenstein number |
| Pe | Péclet number     |
| Pr | Prandtl number    |
| Re | Reynolds number   |

## Subscripts

|     |                  |
|-----|------------------|
| ax  | axial direction  |
| rad | radial direction |
| g   | gas phase        |
| s   | solid phase      |

## A Estimation of the model parameters

In the simulations of the two-dimensional model (4.5)-(4.7), we take the same parameter values as used by Khinast, Jeong and Luss (1999), see Table 2. To compute the effective axial heat

conductivity the following expression is proposed

$$\lambda_{\text{ax}} = (1 - \varepsilon)\lambda_s + \lambda_g + \frac{u^2}{(\rho c_p)_g} h a_v. \quad (\text{A.1})$$

---

|                 |  |                        |  |                      |  |
|-----------------|--|------------------------|--|----------------------|--|
| $(\rho c_p)_s$  | 1382.0 kJ/m <sup>3</sup> K             | $(\rho c_p)_g$         | 0.6244 kJ/m <sup>3</sup> K   | $\eta$               | 1  |
| $k_\infty$      | $9.85 \cdot 10^6 \text{ s}^{-1}$       | $a_v$                  | 1426.0 m <sup>2</sup> <sub>surf</sub> /m <sup>3</sup> <sub>react</sub> | $k_c$                | 0.115 m/s                                  |
| $h$             | 0.02 kW/(m <sup>2</sup> K)             | $L$                    | 4.0 m  | $\varepsilon$        | 0.38                                       |
| $T_c = T_0$     | 323 K                                  | $\Delta T_{\text{ad}}$ | 50 K   | $E_a/R_{\text{gas}}$ | 8328.6 K                                   |
| $D_{\text{ax}}$ | $3 \cdot 10^{-5} \text{ m}^2/\text{s}$ | $\lambda_s$            | 0.0 kW/(mK)  | $\lambda_g$          | $2.6 \cdot 10^{-4} \text{ kW}/(\text{mK})$ |
| $u$             | 1.0 m/s                                | $t_f$                  | 1200s  |                      |  |

---

Table 2: Parameter values for the reverse flow reactor

In this section we derive appropriate values for the radial dispersion  $D_{\text{rad}}$  and for the radial heat conductivity  $\lambda_{\text{rad}}$  using correlation formulas of Westerterp, Swaaij and Beenackers (1988). The derived values of the radial parameters are given in Table 3. In our simulations we fix, in addition, the flow reverse time ( $t_f = 1200\text{s}$ ).

When a fluid flows through a packed bed of solid particles with low porosity, the variations in the local velocity cause a dispersion in the direction of the flow. In not too short beds (i.e.,  $L/d_p > 10$ , where  $d_p$  denotes the particle size) this dispersion can be described by means of a longitudinal dispersion coefficient, although in reality no back mixing occurs. The void spaces of a packed bed can be considered as ideal mixers, and the number of voids is roughly equal to

$$N \sim \frac{L}{d_p}. \quad (\text{A.2})$$

Using the relation  $N = \text{Pe}_m/2 = uL/(2\varepsilon D_{\text{ax}})$ , the following expression for the axial dispersion in packed beds, denoted by the Bodenstein number, can be derived

$$\text{Bo}_{\text{ax}} = \frac{ud_p}{\varepsilon D_{\text{ax}}} = 2. \quad (\text{A.3})$$

To avoid large wall effects, it is assumed that  $d_p/2R < 0.1$ . It is known that the radial Bodenstein number,  $\text{Bo}_{\text{rad}} \sim ud_p/(\varepsilon D_{\text{rad}})$ , approaches a value of 10 to 12 at  $\text{Re} > 100$ . This implies that the coefficient of transverse dispersion  $D_{\text{rad}}$  is about six times smaller than  $D_{\text{ax}}$ .

Heat can be transported perpendicular to the main flow by the same mechanism if a transverse temperature gradient exists, resulting in a convective heat conductivity  $\lambda'_{\text{rad}}$ . Besides, heat transport occurs by thermal radiation between the particles. The (isotropic) thermal conductivity of the bed is denoted by  $\lambda_0$ . The total radial thermal conductivity is then given by

$$\lambda_{\text{rad}} = \lambda_0 + \lambda'_{\text{rad}}, \quad (\text{A.4})$$

where  $\lambda_0$  and  $\lambda'_{\text{rad}}$  act fairly independently. For the convective heat conductivity the following correlation is given

$$\lambda'_{\text{rad}} = \frac{(\rho c_p)_g d_p u}{8[2 - (1 - d_p/R)^2]}. \quad (\text{A.5})$$

Note that under stagnant conditions, we have that  $\lambda'_{\text{rad}} = 0$  and that the radial heat dispersion coefficient equals the thermal conductivity. If the heat diffusion through the solid particles can be neglected, that is,  $\lambda_s = 0$ , the following expression is valid for  $\lambda_0$ , in case of  $0.26 < \varepsilon < 0.93$  and  $T < 673\text{K}$ ,

$$\lambda_0 = 0.67 \cdot \lambda_g \cdot \varepsilon. \quad (\text{A.6})$$

Using the parameter values given in Table 2, we arrive at the following expression for the radial heat conductivity

$$\begin{aligned}\lambda_{\text{rad}} = \lambda_0 + \lambda'_{\text{rad}} &= 6.6 \cdot 10^{-5} + \frac{0.6244 \cdot d_p \cdot 1.0}{8[2 - (1 - d_p/R)^2]} \\ &= 6.6 \cdot 10^{-5} + 7.81 \cdot 10^{-2} \frac{d_p}{2 - (1 - d_p/R)^2}.\end{aligned}$$

If we choose the particle diameter to be  $d_p = 1.0 \cdot 10^{-3}\text{m}$  and take  $R$  in the range from 0.01m to 0.1m, then the radial heat conductivity varies from  $1.32 \cdot 10^{-4}$  to  $1.43 \cdot 10^{-4}$  kW/(mK). Therefore, we can fix the value at  $\lambda_{\text{rad}} = 1.4 \cdot 10^{-4}$  kW/(mK).

---

|       |                             |                  |  |                        |  |
|-------|-----------------------------|------------------|--|------------------------|--|
| $d_p$ | $1.0 \cdot 10^{-3}\text{m}$ | $D_{\text{rad}}$ | $0.5 \cdot 10^{-5} \text{ m}^2/\text{s}$ | $\lambda_{\text{rad}}$ | $1.4 \cdot 10^{-4} \text{ kW}/(\text{mK})$ |
|-------|-----------------------------|------------------|--|------------------------|--|

---

Table 3: Radial parameter value for the two-dimensional model of the reverse flow reactor

## References

- Broyden, C.G. (1965). A class of methods for solving nonlinear simultaneous equations. *Mathematics of Computation*, 19, 577-593.
- Dennis, J.E. & Schnabel, R.B. (1983). *Numerical methods for unconstrained optimization and nonlinear equations*. Prentice-Hall, Englewood Cliffs, NJ.
- Eigenberger, G. & Nieken, U. (1988). Catalytic combustion with periodic-flow reversal. *Chemical Engineering Science*, 43, 2109-2115.
- Gupta, V.K. & Bhatia, S.K.(1991). Solution of cyclic profiles in catalytic reactor operation with periodic-flow reversal. *Computers and Chemical Engineering*, 15, 229-237.
- Iooss, G. & Joseph, D.D.(1990). *Elementary stability and bifurcation theory (2nd ed.)*. New York: Springer-Verlag.
- Khinast, J.G. & Luss, D. (1997) Mapping regions with different bifurcation diagrams of a reverse-flow reactor. *A.I.Ch.E. Journal*, 43, 2034-2047.
- Khinast, J.G., Gurumoorthy, A. & Luss, D. (1998) Complex dynamic features of a cooled reverse-flow reactor. *A.I.Ch.E. Journal*, 44, 1128-1140.
- Khinast, J.G., Jeong, Y.O. & Luss, D. (1999) Dependence of cooled reverse-flow reactor dynamics on reactor model. *A.I.Ch.E. Journal*, 45, 299-309.
- Khinast, J.G. & Luss, D. (2000). Efficient bifurcation analysis of periodically-forced distributed parameter systems. *Computers and Chemical Engineering*, 24, 139-152.
- Lust, K., Roose, D., Spence, A. & Champneys, A.R. (1998). An adaptive Newton-Picard algorithm with subspace iteration for computing periodic solutions. *SIAM Journal on Scientific Computing*, 19, 1188-1209.
- Noorden, T.L. van (2002a). *New algorithms for parameter-swing reactors*. PhD thesis, Vrije Universiteit van Amsterdam.

- Noorden, T.L. van, Verduyn Lunel, S.M. & Blik, A. (2002b). Acceleration of the determination of periodic states of cyclically operated reactors and separators. *Chemical Engineering Science*, *57*, 1041-1055.
- Noorden, T.L. van, Verduyn Lunel, S.M. & Blik, A. (2003). The efficient computation of periodic states of cyclically operated chemical processes. *IMA Journal of Applied Mathematics*, *68*, 149-166.
- Quinta Ferreira, R.M. & Almeida-Costa, C.A. (1996). Heterogeneous models of tubular reactors packed with ion-exchange resins: Simulation of the MTBE synthesis. *Industrial & Engineering Chemistry Research*, *35*, 3827-3841.
- Rehacek, J., Kubicek, M. & Marek, M. (1992). Modeling of a tubular catalytic reactor with flow reversal. *Chemical Engineering Science*, *47*, 2897-2902.
- Rehacek, J., Kubicek, M. & Marek, M. (1998). Periodic, quasiperiodic and chaotic spatiotemporal patterns in a tubular catalytic reactor with periodic flow reversal. *Computers and Chemical Engineering*, *22*, 283-297.
- Rotten, B.A. van de & Verduyn Lunel, S.M. (2003). A limited memory Broyden method to solve high-dimensional systems of nonlinear equations. *Mathematical Institute, Universiteit Leiden*, Technical Report 2003-06.
- Saad, Y. (1992). *Numerical methods for large eigenvalue problems*. Algorithms and Architectures for Advanced Scientific Computing. Manchester: Manchester University Press.
- Westerterp, K.R., Swaaij, W.P.M. van & Beenackers, A.A.C.M. (1988). *Chemical Reactor Design and Operation (2nd ed.)*. John Wiley & Sons Ltd.